



Article

Effect of Coarse Aggregate Grading on Mechanical Parameters and Fracture Toughness of Limestone Concrete

Grzegorz Ludwik Golewski

Department of Structural Engineering, Faculty of Civil Engineering and Architecture, Lublin University of Technology, Nadbystrzycka 40 Str., 20-618 Lublin, Poland; g.golewski@pollub.pl; Tel.: +48-81-5384394; Fax: +48-815-384390

Abstract: This work presents a discussion of the basic properties of broken mineral limestone aggregates with the specification of the properties affecting the fracture toughness of concretes made with these aggregates. To determine the influence of the grain-size distribution of coarse aggregates for each concrete series, two types of aggregate grain were used, with maximum grain sizes of 8 mm (series of concrete L1) and 16 mm (series of concrete L2). Fracture-toughness tests were carried out using mode I fractures in accordance with the RILEM Draft recommendations, TC-89 FMT. During the experiments the critical stress-intensity factor (K_{Ic}^S) and crack-tip-opening displacements ($CTOD_c$) were determined. The main mechanical parameters, i.e., the compressive strength (f_{cm}) and splitting tensile strength (f_{ctm}), were also assessed. Based on the obtained results, it was found that the grain-size distribution of the limestone aggregate influenced the concrete's mechanical and fracture-mechanics parameters. The obtained results showed that the series-L2 concrete had higher strength and fracture-mechanics parameters, i.e.: f_{cm} —45.06 MPa, f_{ctm} —3.03 MPa, K_{Ic}^S —1.22 MN/m^{3/2}, and $CTOD_c$ —12.87 m10⁻⁶. However, the concrete with a maximum grain size of 8 mm (series of concrete L1) presented lower values for all the analyzed parameters, i.e.: f_{cm} —39.17 MPa, f_{ctm} —2.57 MPa, K_{Ic}^S —0.99 MN/m^{3/2}, and $CTOD_c$ —10.02 m10⁻⁶. The main reason for the lower fracture toughness of the concretes with smaller grain sizes was the weakness of the ITZ in this composite compared to the ITZ in the concrete with a maximum grain size of 16 mm. The obtained test results can help designers, concrete producers, and contractors working with concrete structures to ensure the more conscious composition of concrete mixes with limestone aggregates, as well as to produce precise forecasts for the operational properties of concrete composites containing fillers obtained from carbonate rocks.

Keywords: concrete composite; limestone aggregate; grading; brittleness; fracture toughness; interfacial transition zone (ITZ); critical stress-intensity factor (K_{Ic}^S); critical crack-tip-opening displacements ($CTOD_c$)



Citation: Golewski, G.L. Effect of Coarse Aggregate Grading on Mechanical Parameters and Fracture Toughness of Limestone Concrete. *Infrastructures* **2023**, *8*, 117. <https://doi.org/10.3390/infrastructures8080117>

Academic Editor: Bora Pulatsu

Received: 21 June 2023
Revised: 17 July 2023
Accepted: 21 July 2023
Published: 27 July 2023



Copyright: © 2023 by the author. Licensee MDPI, Basel, Switzerland. This article is an open access article distributed under the terms and conditions of the Creative Commons Attribution (CC BY) license (<https://creativecommons.org/licenses/by/4.0/>).

1. Introduction

The achievements of modern concrete technology, enabling the design and production of high-quality concrete with specific performance properties, ensure the leading role of this construction material in construction and infrastructure. Concrete composites with cement matrices are therefore commonly used in the construction of various buildings and structures, for both public and industrial uses. In addition, in recent years, there has also been an increasing use of concretes based on Portland cement for the construction of road surfaces and road-infrastructure facilities. Therefore, increasing numbers of in-depth studies are carried out to assess the specific parameters of this structural material [1–3].

It is necessary to be aware that hardened concrete has a number of properties that significantly determine its behavior under the influence of the load applied. One of the important features that directly affects the durability and safety of concrete structures is the brittleness of the concrete used [4,5]. Moreover, brittleness has a decisive influence on the behavior of the material in places in its structure where defects occur [6–8]. In accordance

with [9], four basic features characterizing the behavior of brittle structural materials can be distinguished:

- When the damage to the structure occurs at the level of average stresses that are significantly lower than the strength of the material;
- If the material does not show clear plastic deformations at room temperature under temporary loading;
- When there is a significant difference between the compressive and the tensile strength of the material;
- In a situation in which a given material is sensitive to stress concentrations, which means that at a critical moment, i.e., with the uncontrolled development of internal microcracks in the material, the local stresses become greater than the average stresses.

Since concrete is one of the materials that shows the signs of brittleness presented above, it is very important to select the components of the concrete mix in a way that reduces the potential for micro-cracking after hardening. As a consequence, such treatments may make it possible to obtain concrete composites with increased fracture toughness [10,11].

As is known, concrete at a given structural level can be considered a two-phase conglomerate, i.e., a material consisting of [12,13]:

- Inclusions—coarse aggregate grains, sand, and unhydrated cement grains;
- A cement matrix as a capillary-porous body—a hardened cement paste in the form of a hydrated mass of cement.

However, the large share of coarse aggregate in the volume of concrete (about 60–80%) inevitably causes the properties of the grains of this filler to affect many of the properties of both young and mature concrete [14]. Therefore, the selection of coarse aggregate requires great care, taking into account both technical and economic factors [15,16].

When analyzing the strength-deformation properties of concrete, it is necessary to consider the properties of the coarse aggregate, as well as interaction between the aggregate and the paste in the interfacial transition zone (ITZ) between them [17,18].

Based on the results of numerous previous studies, it has been shown that it is even necessary to separate the ITZ area as the third basic element of concrete structures [19,20]. The structure, composition, and properties of the paste in this layer are clearly different from those in materials located at a certain distance from the point of contact between the aggregate and the paste [21]. It should also be added that in aggregate grains, especially in those that are coarse, there is a large amount of lattice energy (the energy of the chemical and physico-chemical bonds between the elements of its structure). However, it should be noted that concrete-lattice energy is useless until the structural network of cement stone appears, and until the contact layers between the paste and the aggregate grains are developed. Therefore, it is very important to create compact ITZ areas between the coarse aggregates and the paste. In this phenomenon, during the cement-hydration process, the contact layer is strengthened and aggregate grains are included for interaction with the cement-stone matrix [22,23].

On the other hand, the destruction of structural networks in cement stone and contact layers means the destruction of the concrete. The nature of this destruction depends not only on the tensile strength of the aggregate (the rock from which the aggregate is obtained) and the strength of the cement stone, but also on the characteristics of the ITZ [24–26]. The value of the latter factor for a given cement paste is influenced by the following:

- Type of stone material;
- Level of roughness (smoothness) of the aggregate;
- Size of coarse aggregate grains;
- Degree of cleanliness (dustiness) of the aggregate grain surface;
- Composite curing time.

Therefore, it is very important to know the impact of the type and grading of coarse aggregate on destructive processes in concrete [27–29]. The following article therefore presents the results of experiments and a discussion of the results of fracture toughness

tests of concrete made using one of the most commonly used aggregates in concrete, i.e., limestone aggregate. At this point, it should be noted that the data from the existing literature concerning research of the fracture toughness of concrete with limestone aggregates or other carbonate aggregates are very limited. Only a few articles on this subject have been found in the literature. They concerned:

- Research on the influence of the amount of limestone aggregate on the fracture toughness of concrete at shearing [30];
- Comparison of fracture toughness indicators in limestone concrete with aggregate that has a constant grain size of up to 20 mm in relation to the values of fracture mechanics parameters obtained for gravel concrete, with aggregate that has a maximum grain diameter of 32 mm [31];
- Analysis of fracture mechanics parameters, assessed with the mode II fracture, and microstructure of microcracks in concrete on limestone aggregates [32];
- Fracture toughness tests for three-point bending of concrete with dolomite aggregates [33];
- Tests of fracture toughness of limestone rocks from which an aggregate for the production of concrete is obtained—assessed at static [34] and dynamic loads [35];
- Assessment of the impact of limestone dust content on fracture processes in concrete [36];
- Evaluation of limestone rock fracture processes in I, II, and mixed-fracture models using the Digital Image Correlation (DIC) technique [37];
- Numerical analyses of limestone rock fracture processes [38];
- Tests of fracture toughness of concrete in which part of the cement has been replaced with limestone powder [39];
- Assessment of ITZ microstructure and morphology in concretes with dolomite aggregates [40].

Based on previous studies in the literature, it has been concluded that the problem of the impact of grading of coarse aggregate on fracture processes in concretes made of limestone aggregates is poorly recognized. Available data from the literature contain a wide range of results and conclusions in this regard. There are no precise statements of how the change in the maximum aggregate grain size in the structure of the concrete mix changes the values of the basic parameters of the fracture mechanics in cement concrete.

In order to fill this gap in the scientific literature, experimental research and analysis of the obtained results in the assessment of macroscopic fracture toughness in limestone concretes with different grain sizes of the filler in question have been carried out. Conclusions based on the conducted experiments and analysis of the obtained test results would provide additional information on the impact of the grading of this type of aggregate on changes in both mechanical parameters and fracture mechanics parameters of structural concretes [41,42]. Such knowledge could be helpful for designers, concrete producers, and contractors of concrete structures in [43]:

- A more conscious composing of concrete mixes with limestone aggregates;
- A precise forecasting of the operational properties of concrete composites containing fillers obtained from carbonate rocks.

2. Properties of Limestone Aggregates and Their Application in Construction and Infrastructure—Significance of the Study

Limestone aggregates are representative of crushed stone aggregates. They are obtained from sedimentary carbonate rocks of organic origin. Limestone is usually white, and its dominant component is calcium carbonate, developed in the form of calcite (CaCO_3) and dolomite ($\text{CaCO}_3 \cdot \text{MgCO}_3$) [44].

As a crushed stone aggregate, limestone has many features that favorably affect the properties of concrete. Its texture is rough, and the physical and chemical composition of limestone causes the presence of chemical bonds on its surface, forming a specific diffusion

zone, the thickness of which can range from 20 to 40 μm . As a result, in the case of these aggregates, the structure of compact ITZ is positively affected by both [45]:

- The chemical affinity of limestone aggregate and cement paste;
- The surface roughness of limestone grains.

In the contact zones of limestone aggregates, there is no clear boundary between the two phases of the composite, as is the case with other crushed stone aggregates (e.g., from igneous rocks) and gravel aggregates, but a gradual transition from the filler zone to the cement matrix area. A scheme of the structure of the active contact layer of limestone aggregate with a cement paste is shown in Figure 1.

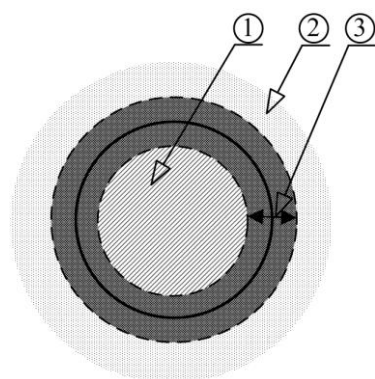


Figure 1. Scheme of the ITZ area between the coarse aggregate and the paste for the chemically reactive limestone aggregate; 1—aggregate grain, 2—cement matrix, and 3—diffusion zone [43].

The above features of carbonate aggregates and additionally their low porosity (up to 4%) have a positive effect on the adhesion between aggregate and cement paste, and cause the formation of more durable and compact contact layers, which have a decisive impact on the processes of brittle fracture in concrete [46,47]. The beneficial effect of chemical adhesion of limestone in concrete has been confirmed in other earlier studies. According to their work [48], the highest adhesion between aggregate and cement paste at a ratio of $w/c = 0.35$ was obtained when limestone aggregates were used in concrete.

Another positive feature is the share of dust from carbonate rocks in the structure of the composite matrix. While in most aggregates an excess of mineral dusts with grain sizes below 0.063 mm adversely affects the direct contact between the cement paste and the aggregate, limestone dusts cause increases in tightness, strength and durability of the concrete [49,50].

Other beneficial features of limestone aggregates also include:

- Low absorbability;
- Good frost resistance;
- Resistance to polishing and surface abrasion.

Therefore, due to their favorable parameters and high availability, carbonate aggregates are now increasingly used as concrete fillers in buildings, bridges and road construction [51]. It is estimated that limestone accounts for about 20% of all crushed stone aggregates used in the concrete industry [52].

In the road industry, this filler is used, e.g., for:

- The production of bituminous mixtures;
- Road foundations for the binding and levelling of wearing courses;
- Renovations and repairs of roads;
- Hardening the surface of alleys and garden paths.

Due to the quite significant use of limestone aggregates in industrial infrastructure, it is necessary to have a thorough knowledge of the processes occurring in the structure of composites made with these fillers. Understanding the quantitative relationships between

the structure and properties of concrete gives the possibility of interfering with the structure of the composite in such a way as to obtain a material with the expected beneficial properties [53,54].

3. Experimental Section

3.1. The Purpose and the Scope of the Research

The use of limestone aggregates for the production of concrete both in various buildings and in the construction of road surfaces caused the need to conduct experimental studies on the impact of the grading of this coarse aggregate on the macroscopic fracture toughness of concrete. As mentioned above, a description of the behavior of brittle materials, such as concrete, requires in-depth knowledge of the basic parameters of fracture mechanics. Such knowledge is helpful in the appropriate selection of a filler, so that the composite is characterized by a reduced content of initial microcracks. Such activities allow for the production of concretes with high values of mechanical parameters and fracture mechanics parameters. This in turn causes an increase in the durability of such materials, and consequently reduces the need for frequent repairs [55].

Therefore, this paper presents the results of experimental research and analyses, concerning the determination of macroscopic fracture toughness according to mode I fracture in cement concretes. In addition, attention was paid to the level of concrete brittleness, which is important in this context [56]. In the course of the experiments conducted, the following basic parameters of fracture mechanics were determined:

- Critical stress intensity factor— K_{Ic}^S ;
- Critical crack tip-opening displacement— $CTOD_c$.

The impact of limestone aggregate grading on the values of the basic strength parameters of the tested composites was also analyzed. In the course of the experiments, the following parameters were evaluated:

- Compressive strength— f_{cm} ;
- Splitting tensile strength— f_{ctm} .

Two series of structural concretes were tested. In order to determine the impact of coarse aggregate grading on the obtained test results, aggregates with a maximum grain diameter of up to 8 mm (L1 series concrete) and up to 16 mm (L2 series concrete) were used.

3.2. Materials

3.2.1. Aggregates

All of the materials used in this study came from Poland. The following types of mineral aggregates were used to prepare concrete mixes for both series of concrete:

- Natural pit sand with 2.0 mm maximum size, from Markuszów deposit—used as fine aggregate;
- Natural broken limestone, often used in the building industry, with 8.0 mm or 16.0 mm maximum size, from Trzuskawica deposit—used as coarse aggregate.

Images of both types of aggregates used are shown in Figure 2.

The main properties of both aggregates used are given in Table 1.

In addition, due to the fact that this article concerns the impact of the grading of the aggregate used on the analyzed parameters, a detailed study of the grading of sand and limestone aggregates was also carried out. The distribution of filler fractions was compiled for both applied coarse aggregate fractions. Aggregate compositions were chosen in such a way that they were contained in the most favorable field between the boundary curves of grading. The study was based on very precise recommendations included in the German standard DIN 4226-1 [57].

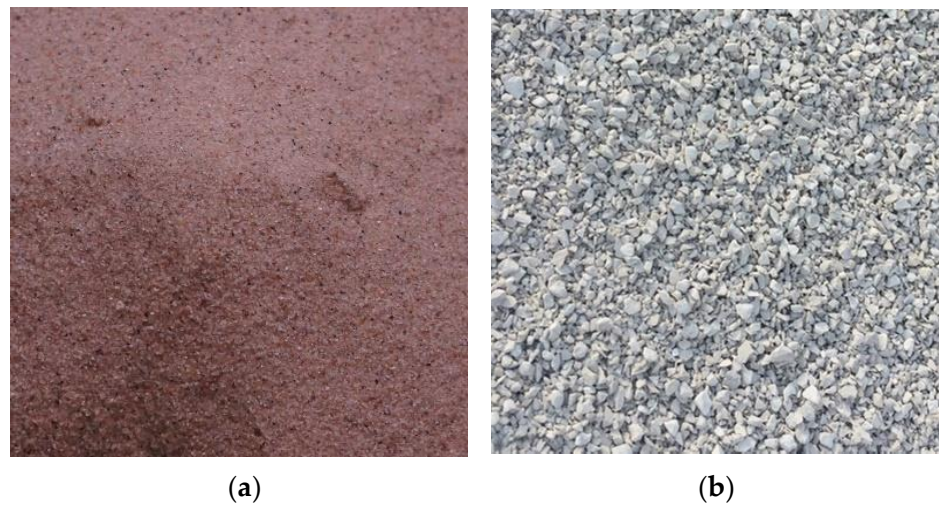


Figure 2. Appearance of aggregates used: (a) sand, and (b) limestone 2–8 mm.

Table 1. Properties of fine and coarse aggregates.

Property	Unit	Aggregate Type	
		Fine Aggregate (Sand)	Coarse Aggregate (Limestone)
Specific Density	(g/cm ³)	2.60	2.85
Bulk Density	(g/cm ³)	2.20	2.70
Compressive Strength	(MPa)	33	100
Modulus of Elasticity	(10 ² MPa)	330	450
Absorption	(%)	0.5	0.3

Concrete in the L1 series was designed from one fraction of coarse aggregate and sand, while concrete in the L2 series was designed from two fractions of coarse aggregate and sand. The exact gradings of aggregates for the concretes in both series are presented in Tables 2 and 3.

Table 2. The particle size distribution of the aggregates used for L1 series concrete.

Fraction (mm)	Content of Aggregate Fraction (%)		
	Sand	Coarse Aggregate, L1	Mix
0–0.125	2.7	0.9	1.6
0.125–0.25	14.9	0.6	5.6
0.25–0.5	42.7	0.5	15.5
0.5–1.0	31.4	1.3	12.1
1.0–2.0	3.9	6.3	5.5
2.0–4.0	4.4	19.3	14.1
4.0–8.0	-	62.2	40.1
8.0–16.0	-	8.9	5.5
Sand point	95.6	9.6	40.3

Table 3. The particle size distribution of the aggregates used for L2 series concrete.

Fraction (mm)	Sand	Coarse Aggregate		Mix
		L2-1	L2-2	
0–0.125	2.5	2.1	0.2	2.1
0.125–0.25	16.2	1.5	0.4	5.1
0.25–0.5	42.2	0.6	-	11.3
0.5–1.0	31.1	1.2	-	10.7
1.0–2.0	5.2	3.8	-	4.1
2.0–4.0	2.8	17.5	-	8.6
4.0–8.0	-	66.8	10.8	33.8
8.0–16.0	-	6.5	88.6	24.2
Sand point	97.2	9.2	0.6	33.3

3.2.2. Binder

The binder used to prepare the concrete mixes was ordinary Portland cement—OPC CEM I 32.5 R—from Chelm cement Plant [58]. The chemical and mineralogical compositions of OPC used are shown in Tables 4 and 5, respectively. It should be noted that the mineralogical composition of the binder was analyzed by the Bogue method. In addition, the main physical properties of OPC are presented in Table 6.

Table 4. Chemical composition of the OPC used (% mass).

Material\Constituent	SiO ₂	Al ₂ O ₃	CaO	MgO	SO ₃	Fe ₂ O ₃	K ₂ O	P ₂ O ₅	TiO ₂	Ag ₂ O
OPC	15.00	2.78	71.06	1.38	4.56	2.72	1.21	-	-	-

Table 5. Mineralogical composition of the OPC used (% mass).

Material\Phase	C ₃ S	C ₂ S	C ₃ A	C ₄ AF	CaSO ₄ (Gypsum)
OPC	60.69	15.82	9.24	7.28	5.10

Table 6. Physical properties of OPC used.

Analyzed Parameter						
Specific Gravity (g/cm ³)	Specific Surface Area (m ² /g)	Average Particle Diameter (μm)	Setting Time (min)		Compressive Strength (MPa)	
			Initial	Final	2 Days	28 Days
3.11	0.33	40.0	207	298	23.3	50.0

3.2.3. Water

In order to prepare concrete mixtures, tap water (W) was used, which met the requirements of standard provision EN 1008:2002 [59].

3.2.4. Admixture

In this study, a calcium lignosulfonate-based plasticizer (P), Basf Liquol BV-18, was used. The plasticizer was used in an amount of 0.6% of mass of the binder in order to improve the flowability of the concrete mixtures.

3.3. Mixture Design, Specimen Preparation and Curing Procedure

The concrete mixture proportions are summarized in Table 7. All mixtures had the same water–binder ratio $w/b = 0.4$.

Table 7. Mix proportions (kg/m³).

Mix	OPC	W	P	Sand	Limestone: L1, 2–8 mm	Limestone: L2-1, 2–8 mm + L2-2, 8–16 mm
L1	352	141	2	676	1207	-
L2	352	141	2	676	-	1207

The samples have been made in a room specifically set aside for sample preparation located at the laboratory of the Faculty of Civil Engineering and Architecture, Lublin University of Technology (Lublin, Poland). The specimens were made in accordance with the EN 12390-2:2019 standard [60]. The process of making concrete mixes was carried out in the DZB-300 counter-rotating mixer with a capacity of 150 L and power of 1.1 kW.

After final preparation, the fresh mixture was poured into molds and compacted on a vibrating table Controls C-161/LC at a frequency of 50 Hz (3000 vibrations/min). After compaction, the upper surface of the specimens was troweled. Then, specimens were placed on the laboratory floor and covered with polyethylene foil. Successive care of the covered specimens was carried out by additional wetting every few hours.

The following concrete specimens were prepared for the experimental tests:

- Cubes for evaluating mechanical parameters f_{cm} and f_{ctm} ;
- Beams with one initial crack to assess the fracture toughness parameters K_{IC}^S and $CTOD_c$.

The specimens were demolded 48 h after their preparation, and then transferred to a tub filled with water, with automatic stabilization of temperature conditions. In this way, they have been kept in water for 14 days. After this period, the specimens were taken out of the water and placed on wooden pallets, where they remained for another 14 days, until macroscopic examinations were carried out. During this period, specimens were cured in laboratory conditions at $t = 20 \pm 2$ °C and RH = 40% [60]. Details of specimen preparation for fracture toughness tests are given in Section 3.4.2.

3.4. Test Procedures

3.4.1. Examinations of Mechanical Parameters

Tests of concrete strength parameters were carried out in a static manner on a computer-controlled strength machine with a maximum pressure force of 3000 kN. To determine f_{cm} and f_{ctm} , cubic samples with a side length of 150 mm were used. For each type of test and each batch of concrete, 6 samples were used. Characteristics of the most relevant data related to strength tests are presented in Table 8.

Table 8. The main data regarding mechanical parameter examinations.

Parameter Type	Parameter Characteristics
Testing machine used in the study	Walter + Bai AG hydraulic servo testing machine
The shape of the specimens	Cube
Specimens' dimensions	150 × 150 × 150 mm
Studies that used specimens	<ul style="list-style-type: none"> • Compressive strength; • Splitting tensile strength.
Number of specimens	6 specimens for each test and each series of concrete
Type of specimen load	Static
Standards used in the studies	<ul style="list-style-type: none"> • EN 12390-3:2011 + AC:2012 [61]—in the case of compression strength—f_{cm}; • EN 12390-6:2009 [62]—in the case of splitting tensile strength—f_{ctm}.

3.4.2. Fracture Toughness Investigations

In this research, in order to evaluate the fracture mechanics parameters of concrete composites, i.e., K_{Ic}^S and $CTODc$, for each mixture, 6 notched beams with the same dimensions $80 \times 150 \times 700$ mm (depth \times width \times length) with a span of 600 mm were made (Figure 3).

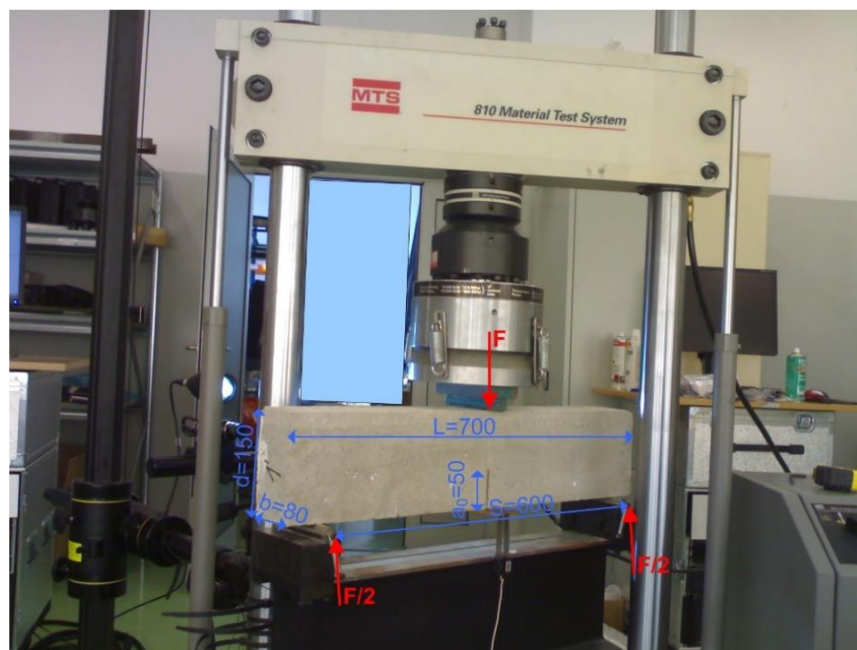


Figure 3. View of specimen (including load scheme and dimensions in mm) during fracture toughness tests.

Figure 3 shows a sample of concrete beams tested for fracture toughness analysis. The initial vertical notch with a constant width of 3 mm was created by placing a steel plate in the middle of the beam in the tensile direction of the specimens (Figure 3).

The fracture toughness test was carried out in accordance with the RILEM Draft recommendations TC-89 FMT [63] using MTS 810 testing machine (Figure 3). In addition, the crack opening sensor, which was the MTS clip gage axial extensometer 632,03F-3, was used in order to measure width of the initial crack opening during the tests (Figure 3). During the tests carried out on the MTS 810 press, Force (F)–crack mouth opening displacement ($CMOD$) curves were recorded.

The analyzed fracture toughness K_{Ic}^S and $CTODc$ were determined with the use of obtained diagrams, F – $CMOD$, and the detailed formulas given in [63]. It should be added that in order to determine fracture mechanics parameters, it was necessary to read the following data from the F – $CMOD$ charts:

- Maximum load obtained in the tests, marked in red (F_{max});
- Tangent in the first phase of the F – $CMOD$ relationship, highlighted in blue (C_i);
- Tangent in the second phase of the F – $CMOD$ relationship, highlighted in yellow (C_u).

They have been marked on the exemplary charts for each of the analyzed composites.

4. Results and Discussion

4.1. Mechanical Parameters

The obtained average mechanical parameters $\overline{f_{cm}}$ and $\overline{f_{ctm}}$ are shown in Tables 9 and 10, respectively. Statistical parameters, i.e., the standard deviation— δ and coefficient of variation— ν , as well as the spread of the results (max. and min. values) are also given in these tables.

Table 9. Results of compressive strength f_{cm} .

Mix	$\overline{f_{cm}}$ (MPa)	δ (MPa)	ν (%)	$f_{cm'} \text{ Max.}$ (MPa)	$f_{cm'} \text{ Min.}$ (MPa)
L1	39.17	1.09	2.8	42.15	37.88
L2	45.06	2.57	5.7	47.18	43.62

Table 10. Results of splitting tensile strength f_{ctm} .

Mix	$\overline{f_{ctm}}$ (MPa)	δ (MPa)	ν (%)	$f_{ctm'} \text{ Max.}$ (MPa)	$f_{ctm'} \text{ Min.}$ (MPa)
L1	2.57	0.15	5.7	2.81	2.25
L2	3.03	0.2	6.2	3.23	2.87

On the basis of the obtained results, it can be concluded that the size of grains in the limestone aggregate used has a direct impact on the basic strength parameters of the concrete composite. A significant improvement in the results of strength tests, both f_{cm} and f_{ctm} , was observed when using aggregates with a larger grading.

It was observed that, for the concrete in series L2, the compressive strength of the composite is 45.06 MPa, indicating an increase of 15% compared with the working condition of the concrete in series L1 (Table 9). On the other hand, the corresponding splitting tensile strength is 3.03 MPa, indicating an increase of 18% compared with the working condition for series L1 concrete (Table 10).

4.2. Fracture Toughness

The exemplary F - $CMOD$ curves of the concrete beams, prepared with limestone aggregates with different grading, under three-point flexural loads are shown in Table 11 [64,65]. Important data, such as F_{max} , C_i , and C_u , are also shown in each of the exemplary charts.

Table 11. Exemplary F - $CMOD$ curves with significant details for analyzed composites.

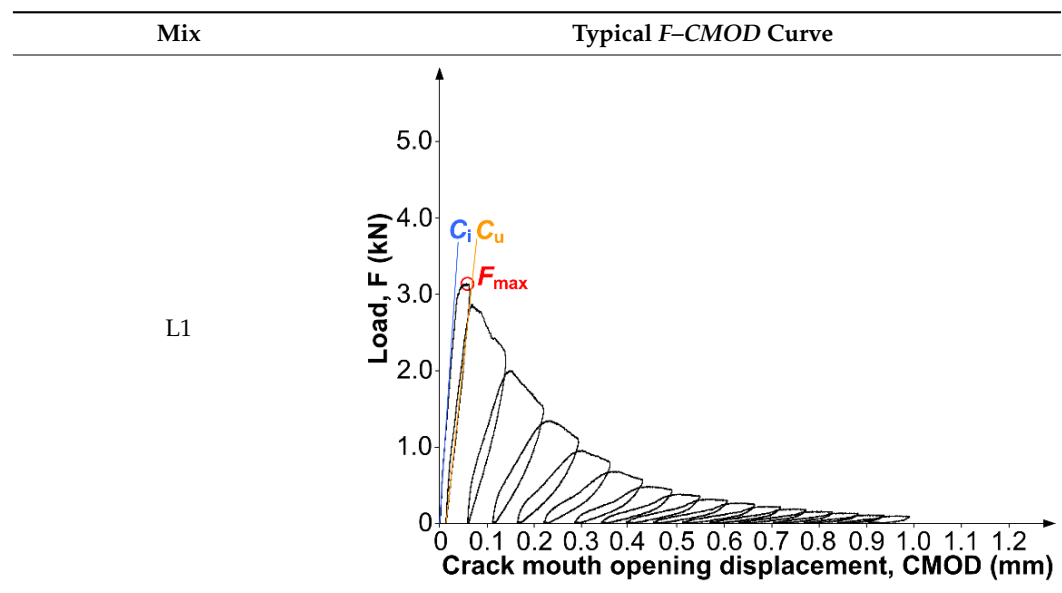
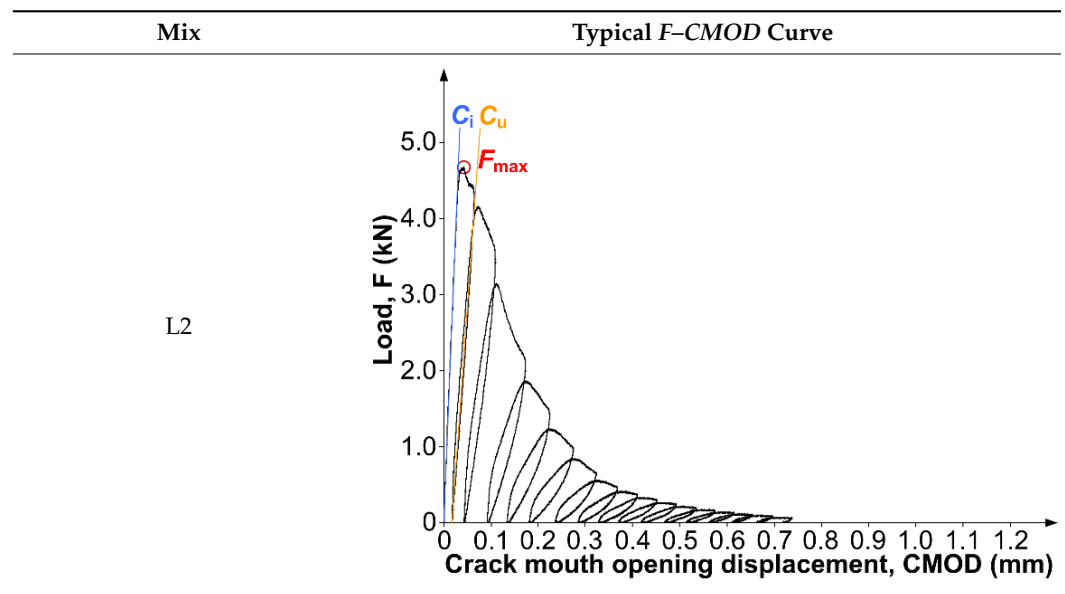


Table 11. Cont.



On the basis of the compiled graphs in Table 11, it can be concluded that the specimens in all concretes were damaged at the F_{max} force, which was:

- About 3.0 kN for series L1 concrete, i.e., with a maximum grain size of up to 8 mm;
- Almost 5.0 kN for series L2 concrete, i.e., with a maximum grain size of up to 16 mm.

In addition, by analyzing the slope of the F - $CMOD$ curves, assessed on the basis of the shape of the C_i and C_u tangents, it can be concluded that the proposed modification of composite structure, i.e., the change in the grain size of the coarse aggregate, also changed the behavior of the composites in the process of their destruction. The smallest changes were those observed in L2 series concrete. In addition, the initial crack development process, visible on the load-unload loops, was relatively short in this composite. In the case of cyclic material damage, the effect of its “flow” was not observed. However, such behavior was clearly visible for the composite in the Mix-L1 series (Table 11). This proves that the concrete in the Mix-L2 series was more brittle than both of the analyzed composites [66,67].

The observed average fracture toughness $\overline{K_{Ic}^S}$ and $\overline{CTOD_c}$ are shown in Tables 12 and 13, respectively. Statistical parameters, i.e., the standard deviation— δ and coefficient of variation— ν , as well as the spread of the results (max. and min. values), are also given in these tables.

Table 12. Results of critical stress intensity factor K_{Ic}^S .

Mix	$\overline{K_{Ic}^S}$ (MN/m ^{3/2})	δ (MN/m ^{3/2})	ν	$\overline{K_{Ic}^S}$, Max. (MN/m ^{3/2})	$\overline{K_{Ic}^S}$, Min. (MN/m ^{3/2})
L1	0.99	0.13	8.98	1.28	0.76
L2	1.22	0.18	7.08	1.38	1.06

Table 13. Results of critical crack-tip-opening displacement $CTOD_c$.

Mix	$\overline{CTOD_c}$ (m10 ⁻⁶)	δ (MPa)	ν	$CTOD_c$, Max. (m10 ⁻⁶)	$CTOD_c$, Min. (m10 ⁻⁶)
L1	10.02	1.28	8.76	13.16	8.45
L2	12.87	3.29	7.25	15.13	10.22

On the basis of the obtained results of fracture mechanics parameters, it can be concluded that, similarly to the results of strength parameters, a change in the applied limestone

aggregate grading also had a clear impact on the fracture toughness. Moreover, in this case, a much more pronounced improvement in the results of the analyzed parameters $CTOD_c$ and K_{Ic}^S was observed when using limestone aggregates with a maximum grain size of up to 16 mm.

It was observed that, for the concrete in series L2, the critical stress intensity factor K_{Ic}^S is $1.22 \text{ MN/m}^{3/2}$, indicating an increase of 23% compared with the working condition of concrete in series L1 (Table 12). However, the critical crack-tip-opening displacement is $12.87 \text{ m}10^{-6}$, indicating an increase of up to 28% compared with the working condition in series L1 concrete (Table 13).

In order to further analyze the differences in the structure of the tested concretes, macroscopic observations of their fractures in cross-sections were made, where sharpened flat bars modeling the shape of the initial crack were placed [68,69]. Observations of the surface structure of fractures had been previously correlated with the fracture toughness, among others, by the authors of the work [70]. In their experiments, they examined three-point bent beams with a preliminary notch with three different geometric dimensions and a variable composition of concrete mixtures. They compared concretes made of aggregates with a maximum grain diameter of 6 and 25 mm. As a result of the analyses contained therein, it was determined that the macroscopic assessment of the damaged concrete structure may be helpful in explaining the reasons for the obtained values of fracture mechanics parameters. Therefore, it was considered that such analysis could be helpful in explaining the favorable results obtained when using the limestone coarse aggregate with a higher grading.

Figure 4 shows two exemplary cross-sections of the analyzed concrete beams. In macroscopic tests of sample fractures, it was found that the paste structure in L2 series concrete is tight and compact, with a regular structure and small number of microcracks at the contact area of the aggregate grains and cement paste. More damage, especially in the area of the contact layer of the coarse aggregate with the cement matrix, could be observed in composites with lower grading, i.e., the L1 series.

This was also confirmed by the results of microscopic tests performed using the XC-100 L optical microscope—shown at the top of the cross-sections in Figure 4. On this basis, selected examples of ITZ of both concrete series were evaluated.

Such results of visual inspection allow us to conclude that the fracture toughness of concrete made with limestone aggregates is mainly determined by the cohesion forces in the layer at the aggregate–paste boundary. In the fractures of the L1 series beams, small decohesive cracks, probably formed in the process of concrete curing, were observed. On the surface of the cross-section, minor microcracks in the composite structure were also visible, indicating a worse adhesion in the ITZ area [71–74]. This is clearly visible under microscopic magnification (Figure 4a).

A larger area of the limestone aggregate with a grain size of up to 16 mm resulted in the creation of a larger area of diffusion zones in the material structure (Figure 1). Therefore, the ITZ zone in this composite was more compact compared to the concrete samples in the L1 series (Figure 4b). This in turn caused a delay in the destructive processes in the material, which is clearly visible in the graphs presented in Table 12. As a result, an increase in both strength characteristics and the parameters of the fracture mechanics in L2 series concrete (Tables 9–13) was observed.

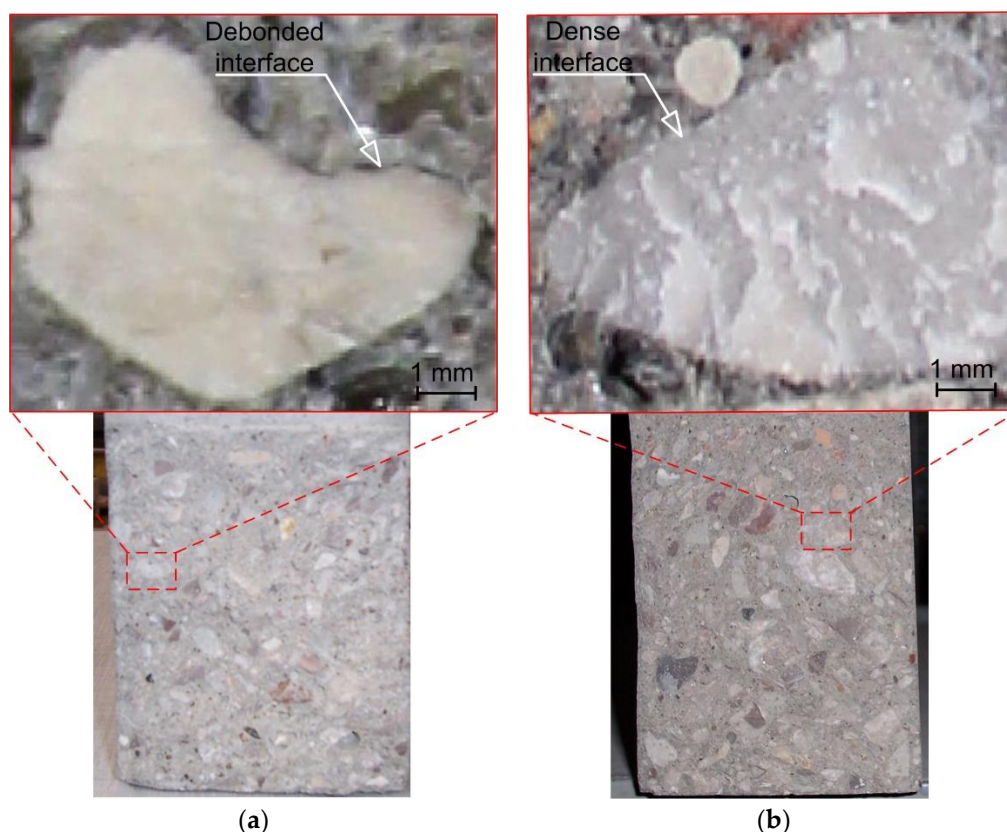


Figure 4. Cross-section of analyzed concrete composites after fracture toughness test with visible characteristic macroscopic structure and exemplary microscopic images of damaged aggregates: (a) L1, and (b) L2; description in the text.

5. Summary and Conclusions

In the course of the conducted research, it was found that concretes made with limestone aggregates with a grain size of up to 16 mm had a higher fracture toughness than concretes containing aggregates of the same type with a maximum grain diameter of up to 8 mm. Increases in both analyzed parameters of the fracture mechanics were in favor of the L2 series concrete, respectively:

- 23% in the case of K_{Ic}^S ;
- 28% in the case of $CTOD_c$.

These results were matched with the analyzed strength parameters. Also, in this case, higher values were observed (although not so clearly) for concretes with a higher grading. It was determined that they increased after changing the grading of the limestone aggregate from a maximum grain size of 8 mm to 16 mm. They increased by:

- 15% in the case of f_{cm} ;
- 18% in the case of f_{ctm} .

Therefore, it can be concluded that results of the strength parameters tests, f_{cm} and f_{ctm} , are similar qualitatively to the obtained results of the fracture toughness tests, K_{Ic}^S and $CTOD_c$.

After macroscopic analysis of the cross-sections of concrete samples after their destruction, it can be concluded that the main reason for both a lower fracture toughness and a reduced strength of concretes with lower grain size is the weaker contact layer in these composites. Worse adhesion of smaller aggregate inclusions to the matrix resulted in faster development of damage in the form of decohesion in the ITZ area of the phases.

In L1 concrete, small grains prevented the formation of a compact composite structure with a good fracture toughness. This led to the formation, under the acting load, of a greater

number of micro-discontinuities, i.e., a faster destruction of the concrete. As a result, the concrete was weaker and had a lower fracture toughness (Tables 9–13).

Analyzing the exemplary F – $CMOD$ curves compiled in Table 12, it can be concluded that in the case of the L1 series concrete, they showed the features of quasi-plastic deformations. On the other hand, concrete with a higher grading behaved like brittle material during the ongoing destruction process.

Taking into account the results of the research carried out, it can be concluded that:

1. Concretes made of limestone aggregates with a maximum aggregate grain size up to 16 mm are characterized by increases in strength values f_{cm} and f_{ctm} , of several percent to 20%, compared to concretes containing the same type of coarse aggregate with a smaller grain size of up to 8 mm (Tables 9 and 10).
2. Fracture toughness of concretes with limestone aggregates is significantly higher, by 20% to even 30%, when using a mixture of aggregates with higher grading (Tables 12 and 13).
3. The results of the main strength parameters of limestone concretes are qualitatively similar to the fracture toughness results obtained for these composites (Tables 9–13).
4. Concretes with limestone aggregates with a maximum grain size of up to 16 mm behave like brittle materials during the ongoing destruction process. However, in concretes with a maximum grain size of up to 8 mm, signs of quasi-plasticity are visible during their destruction process (Table 11).
5. Due to intensified feature for creating a diffusion zone in the ITZ area, larger grains of limestone aggregates are able to produce more compact contact points between coarse aggregate grains and the paste (Figure 4). This had a decisive impact on the obtained favorable strength parameters and fracture mechanics parameters in the L2 series concrete.
6. The use of the research results presented in this study may be helpful in designing the composition of concrete mixtures with limestone aggregates with a focus on improving their fracture toughness. This, in turn, may contribute to obtaining a construction material with a reduced number of initial defects in the ITZ zone. Increases in mechanical parameters of concrete and an improvement of its fracture toughness will consequently lead to an increase in the reliability of concrete structures made of such materials.

Funding: This research received no external funding.

Institutional Review Board Statement: Not applicable.

Informed Consent Statement: Not applicable.

Data Availability Statement: No new data were created or analyzed in this study. Data sharing is not applicable to this article.

Conflicts of Interest: The author declares no conflict of interest.

References

1. Liu, F.; Zou, Y.; Wang, B.; Yuan, X. The Effect of Stray Current on Calcium Leaching of Cement-Based Materials. *Materials* **2022**, *15*, 2279. [[CrossRef](#)]
2. Wardach, M.; Krentowski, J.R.; Mackiewicz, M. Evaluation of Precast Beam Deflections Resulting in Cracks in Curtain Walls. *Eng. Fail. Anal.* **2022**, *140*, 106568. [[CrossRef](#)]
3. Golewski, G.L. The Specificity of Shaping and Execution of Monolithic Pocket Foundations (PF) in Hall Buildings. *Buildings* **2022**, *12*, 192. [[CrossRef](#)]
4. Zhang, S.; Han, B.; Xie, H.; An, M.; Lyu, S. Brittleness of Concrete under Different Curing Conditions. *Materials* **2021**, *14*, 7865. [[CrossRef](#)]
5. Yao, W.; Pang, J.; Liu, Y. An Experimental Study of Portland Cement and Superfine Cement Slurry Grouting in Loose Sand and Sandy Soil. *Infrastructures* **2018**, *3*, 9. [[CrossRef](#)]
6. Kovacic, J.; Marsavina, L.; Linul, E. Poisson's Ratio of Closed-Cell Aluminum Foams. *Materials* **2018**, *11*, 1904. [[CrossRef](#)]

7. Zhang, P.; Wang, C.; Gao, Z.; Wang, F. A Review on Fracture Properties of Steel Fiber Reinforced Concrete. *J. Build. Eng.* **2023**, *67*, 105975. [[CrossRef](#)]
8. Craciun, E.M. Energy Criteria for Crack Propagation in Prestresses Elastic Composites. *Sol. Mech. Appl.* **2008**, *154*, 193–237.
9. Golewski, G.L. The Phenomenon of Cracking in Cement Concretes and Reinforced Concrete Structures: The Mechanism of Cracks Formation, Causes of Their Initiation, Types and Places of Occurrence, and Methods of Detection—A Review. *Buildings* **2023**, *13*, 765. [[CrossRef](#)]
10. Kibriya, G.; Orosz, Á.; Botzheim, J.; Bagi, K. Calibration of Micromechanical Parameters for the Discrete Element Simulation of a Masonry Arch using Artificial Intelligence. *Infrastructures* **2023**, *8*, 64. [[CrossRef](#)]
11. Vuoto, A.; Funari, M.F.; Lourenço, P.B. On the Use of the Digital Twin Concept for the Structural Integrity Protection of Architectural Heritage. *Infrastructures* **2023**, *8*, 86. [[CrossRef](#)]
12. Golewski, G.L.; Szostak, B. Strength and Microstructure of Composites with Cement Matrixes Modified by Fly Ash and Active Seeds of C-S-H Phase. *Struct. Eng. Mech.* **2022**, *82*, 543–556.
13. Craciun, E.M.; Carabineanu, A.; Peride, N. Antiplane Interface Crack in a Pre-Stressed Fiber-Reinforced Elastic Composite. *Comp. Mater. Sci.* **2008**, *43*, 184–189. [[CrossRef](#)]
14. Fournari, R.; Ioannou, I. Correlations between the Properties of Crushed Fine Aggregates. *Minerals* **2019**, *9*, 86. [[CrossRef](#)]
15. Gil, D.M.; Golewski, G.L. Potential of Siliceous Fly Ash and Silica Fume as a Substitute of Binder in Cementitious Concrete. *E3S Web Conf.* **2018**, *49*, 00030. [[CrossRef](#)]
16. Golewski, G.L. Study of Strength and Microstructure of a New Sustainable Concrete Incorporating Pozzolan Materials. *Struct. Eng. Mech.* **2023**, *86*, 431–441.
17. Kong, Y.; Wang, P.; Liu, S.; Zhao, G.; Peng, Y. SEM Analysis of the Interfacial Transition Zone between Cement-Glass Powder Paste and Aggregate of Mortar under Microwave Curing. *Materials* **2016**, *9*, 733. [[CrossRef](#)]
18. Golewski, G.L. Concrete Composites Based on Quaternary Blended Cements with a Reduced Width of Initial Microcracks. *Appl. Sci.* **2023**, *13*, 7338. [[CrossRef](#)]
19. Imtiaz, T.; Ahmed, A.; Hossain, M.S.; Faysal, M. Microstructure Analysis and Strength Characterization of Recycled Base and Sub-Base Materials Using Scanning Electron Microscope. *Infrastructures* **2020**, *5*, 70. [[CrossRef](#)]
20. Hashemmoniri, S.; Fatemi, A. Optimization of Lightweight Foamed Concrete Using Fly Ash Based on Mechanical Properties. *Inn. Infr. Sol.* **2023**, *8*, 59. [[CrossRef](#)]
21. Golewski, G.L. Studies of Natural Radioactivity of Concrete with Siliceous Fly Ash Addition. *Cem. Wapno Beton* **2015**, *2*, 106–114.
22. Wang, L.; Zhang, P.; Golewski, G.L.; Guan, J. Editorial: Fabrication and Properties of Concrete Containing Industrial Waste. *Front. Mater.* **2023**, *10*, 1169715.
23. Golewski, G.L. The Effect of the Addition of Coal Fly Ash (CFA) on the Control of Water Movement within the Structure of the Concrete. *Materials* **2023**, *16*, 5218. [[CrossRef](#)]
24. Wei, J.; Liu, J.; Khayat, K.H.; Long, W.-J. Synergistic Effect of HEDP.4Na and Different Induced Pouring Angles on Mechanical Properties of Fiber-Reinforced Alkali-Activated Slag Composites. *Fibers* **2023**, *11*, 23. [[CrossRef](#)]
25. Golewski, G.L.; Sadowski, T. Macroscopic Evaluation of Fracture Processes in Fly Ash Concrete. *Solid State Phenom.* **2016**, *254*, 188–193. [[CrossRef](#)]
26. Reis, J.M.L.; Chianelli-Junior, R.; Cardoso, J.L.; Marinho, F.J.V. Effect of Recycled PET in the Fracture Mechanics of Polymer Mortar. *Constr. Build. Mater.* **2011**, *25*, 2799–2804. [[CrossRef](#)]
27. Li, X.; Zhang, Q. Influence Behavior of Phosphorus Slag and Fly Ash on the Interface Transition Zone in Concrete Prepared by Cement-Red Mud. *J. Build. Eng.* **2021**, *49*, 104017. [[CrossRef](#)]
28. Golewski, G.L.; Sadowski, T. A Study on Mode III Fracture Toughness in Young and Mature Concrete with Fly Ash Additive. *Solid State Phenom.* **2016**, *254*, 120–125. [[CrossRef](#)]
29. Prokopski, G. Effect of Coarse Aggregate Quantity on Fracture Toughness of Concretes. *J. Mater. Sci.* **1993**, *28*, 5717–5721. [[CrossRef](#)]
30. Hordijk, D.A.; Wolsink, G.M.; de Vries, J. Fracture and Fatigue Behaviour of a High Strength Limestone Concrete as a Compared to Gravel Concrete. *Heron* **1995**, *40*, 125–146.
31. Golewski, G.; Sadowski, T. Fracture Toughness at Shear (Mode II) of Concretes Made of Natural and Broken Aggregates. *Brittle Matrix Compos.* **2006**, *8*, 537–546.
32. Prokopski, G.; Halbiniak, J. Interfacial Transition Zone in Cementitious Materials. *Cem. Concr. Res.* **2000**, *30*, 579–583. [[CrossRef](#)]
33. Schmidt, R.A. Fracture-Toughness Testing of Limestone. *Exp. Mech.* **1976**, *16*, 161–167. [[CrossRef](#)]
34. Iha, A.K. Dynamic Fracture Toughness Test of Limestone. *J. Geol. Res. Eng.* **2020**, *8*, 184–196.
35. Qi, J.; Jiang, L.; Zhu, M.; Mu, C.; Li, R. Experimental Study on the Effect of Limestone Powder Content on the Dynamic and Static Mechanical Properties of Seawater Coral Aggregate Concrete (SCAC). *Materials* **2023**, *16*, 3381. [[CrossRef](#)]
36. Helmer, G.S.; Sulem, J.; Ghabezloo, S.; Rohmer, J.; Hild, F. Experimental Evaluation of the Fracture Toughness on a Limestone. In Proceedings of the ISRM Regional Symposium—EUROCK 2014, Vigo, Spain, 26–28 May 2014.
37. Singh, R.N.; Sun, G. A Numerical and Experimental Investigation for Determining Fracture Toughness of Welsh Limestone. *Min. Sci. Technol.* **1990**, *10*, 61–70. [[CrossRef](#)]
38. Menadi, B.; Kenai, S.; Khatib, J.M. Fracture Behaviour of Concrete Containing Limestone Fines. *Proc. Inst. Civ. Eng.—Constr. Mater.* **2014**, *167*, 162–170. [[CrossRef](#)]

39. Prokopski, G.; Halbiniak, J.; Langier, B. The Examination of the Fracture Toughness of Concretes with Diverse Structure. *J. Mater. Sci.* **1998**, *33*, 1819–1825. [[CrossRef](#)]
40. Golewski, G.L. An Analysis of Fracture Toughness in Concrete with Fly Ash Addition, Considering All Models of Cracking. *IOP Conf. Ser. Mater. Sci. Eng.* **2018**, *416*, 012029. [[CrossRef](#)]
41. Bochenek, A.; Prokopski, G.B. The Investigation of Aggregate Grain Size Effect on Fracture Toughness of Ordinary Concrete Structures. *Int. J. Fract.* **1989**, *41*, 197–205. [[CrossRef](#)]
42. Golewski, G.L.; Sadowski, T. Experimental Investigation and Numerical Modelling Fracture Processes in Fly Ash Concrete at Early Age. *Solid State Phenom.* **2012**, *188*, 158–163. [[CrossRef](#)]
43. Carlos, A.; Masumi, I.; Hiroaki, M.; Maki, M.; Takahisa, O. The Effects of Limestone Aggregate on Concrete Properties. *Constr. Build. Mater.* **2010**, *24*, 2363–2368.
44. Neville, A.M. *Properties of Concrete*; Pearson Education Limited: Harlow, UK, 2011.
45. Aghajanian, A.; Cimentada, A.; Fayyaz, M.; Brand, A.S.; Thomas, C. ITZ Microanalysis of Cement-based Building Materials with Incorporation of Siderurgical Aggregates. *J. Build. Eng.* **2023**, *67*, 106008. [[CrossRef](#)]
46. Golewski, G.L. Fracture Performance of Cementitious Composites Based on Quaternary Blended Cements. *Materials* **2022**, *15*, 6023. [[CrossRef](#)]
47. Van Mier, J.G.M. *Fracture Processes of Concrete: Assessment of Material Parameters for Fracture Models*; CRC Press: Boca Raton, FL, USA; New York, NY, USA; London, UK; Tokyo, Japan, 2000.
48. Sun, Z.; Xiong, J.; Cao, S.; Zhu, J.; Jia, X.; Hu, Z.; Liu, K. Effect of Different Fine Aggregate Characteristics on Fracture Toughness and Microstructure of Sand Concrete. *Materials* **2023**, *16*, 2080. [[CrossRef](#)]
49. Golewski, G.L. The Role of Pozzolanic Activity of Siliceous Fly Ash in the Formation of the Structure of Sustainable Cementitious Composites. *Sustain. Chem.* **2022**, *3*, 520–534. [[CrossRef](#)]
50. Ghafoori, N.; Spitek, R.; Najimi, M. Influence of Limestone Size and Content on Transport Properties of Self-Consolidating Concrete. *Constr. Build. Mater.* **2016**, *127*, 588–595. [[CrossRef](#)]
51. Lewicka, E.; Szigaj, J.; Burkowicz, A.; Galos, K. Sources and Markets of Limestone Flour in Poland. *Resources* **2020**, *9*, 118. [[CrossRef](#)]
52. Golewski, G.L. Combined Effect of Coal Fly Ash (CFA) and Nanosilica (Ns) on the Strength Parameters and Microstructural Properties of Eco-Friendly Concrete. *Energies* **2023**, *16*, 452. [[CrossRef](#)]
53. Xie, T.; Yang, G.; Zhao, X.; Xu, J.; Fang, C. A Unified Model for Predicting the Compressive Strength of Recycled Aggregate Concrete Containing Supplementary Cementitious Materials. *J. Clean. Prod.* **2020**, *251*, 119752. [[CrossRef](#)]
54. Jwaida, Z.; Dulaimi, A.; Mashaan, N.; Othuman Mydin, M.A. Geopolymers: The Green Alternative to Traditional Materials for Engineering Applications. *Infrastructures* **2023**, *8*, 98. [[CrossRef](#)]
55. Golewski, G.L. Mechanical Properties and Brittleness of Concrete Made by Combined Fly Ash, Silica Fume and Nanosilica with ordinary Portland cement. *AIMS Mater. Sci.* **2023**, *10*, 390–404. [[CrossRef](#)]
56. *DIN 4226-1:2001-07*; Aggregates for Concrete and Mortar—Part 1: Normal and Heavy-Weight Aggregates. German Standards Institution: Essen, Germany, 2001.
57. *EN 197-1:2011*; Cement—Part 1: Composition, Specifications and Conformity Criteria for Common Cements. NSAI Standard: Dublin, Ireland, 2011.
58. *EN 1008:2002*; Mixing Water for Concrete—Specification for Sampling, Testing and Assessing the Suitability of Water, Including Water Recovered from Processes in the Concrete Industry, as Mixing Water for Concrete. British Standards Institution (BSI): London, UK, 2002.
59. *EN 12390-2:2019*; Testing Hardened Concrete—Part 2: Making and Curing Specimens for Strength Tests. British Standards Institution (BSI): London, UK, 2019.
60. *EN 12390-3: 2011+AC*; Testing Hardened Concrete—Part 3: Compressive Strength of Test Specimens. British Standards Institution (BSI): London, UK, 2012.
61. *EN 12390-6: 2009*; Testing Hardened Concrete—Part 6: Tensile Splitting Strength of Test Specimens. British Standards Institution (BSI): London, UK, 2009.
62. Shah, S.P. Determination of fracture parameters (K_{Ic}^S and $CTOD_c$) of plain concrete using three-point bend tests, RILEM Draft Recommendations, TC 89-FMT Fracture Mechanics of Concrete Test Methods. *Mater. Struct.* **1990**, *23*, 457–460. [[CrossRef](#)]
63. Hu, H.; Huang, Y.; Zhao, L.; Xiong, M. Shaking Table Tests on Slope Reinforced by Anchored Piles under Random Earthquake Ground Motions. *Acta Geot.* **2022**, *17*, 4113–4130. [[CrossRef](#)]
64. Bao, Y.; Hu, H.; Gan, G. Seismic Response Analysis of Slope Reinforced by Pile-Anchor Structures under Near-Fault Pulse-like Ground Motions. *Soil Dynam. Earth. Eng.* **2023**, *164*, 107576. [[CrossRef](#)]
65. Golewski, G.L. Comparative Measurements of Fracture Toughness Combined with Visual Analysis of Cracks Propagation Using the DIC Technique of Concretes Based on Cement Matrix with a Highly Diversified Composition. *Theor. Appl. Fract. Mech.* **2022**, *121*, 103553. [[CrossRef](#)]
66. Golewski, G.L. An Extensive Investigations on Fracture Parameters of Concretes Based on Quaternary Binders (QBC) by Means of the DIC Technique. *Constr. Build. Mater.* **2022**, *351*, 128823. [[CrossRef](#)]
67. Pena-Caballero, C.; Kim, D.; Gonzalez, A.; Castellanos, O.; Cantu, A.; Ho, J. Real-Time Road Hazard Information System. *Infrastructures* **2020**, *5*, 75. [[CrossRef](#)]

68. Wu, J.; Yang, J.; Zhang, R.; Jin, L.; Du, X. Fatigue Life Estimating for Chloride Attacked RC Beams Using S-N Curve Combined with Mesoscale Simulation of Chloride Ingress. *Int. J. Fat.* **2022**, *158*, 106751. [[CrossRef](#)]
69. Perdikaris, P.C.; Romeo, A. Size Effect on Fracture Energy of Concrete and Stability Issues in Three-Point Bending Fracture Toughness Testing. *ACI Mater. J.* **1995**, *92*, 483–496.
70. Golewski, G.L. Changes in the Fracture Toughness under Mode II Loading of Low Calcium Fly Ash (LCFA) Concrete Depending on Ages. *Materials* **2020**, *13*, 5241. [[CrossRef](#)] [[PubMed](#)]
71. Zhang, B.; Zhu, H.; Lu, F. Fracture Properties of Slag-Based Alkali-Activated Seawater Coral Aggregate. *Theor. Appl. Fract. Mech.* **2019**, *115*, 103071. [[CrossRef](#)]
72. Peride, N.; Carabineanu, A.; Craciun, E.M. Mathematical Modelling of the Interface Crack Propagation in a Pre-Stressed Fiber Reinforced Elastic Composite. *Comp. Mater. Sci.* **2009**, *45*, 684–692. [[CrossRef](#)]
73. Linul, E.; Marsavina, L.; Valean, C.; Banica, R. Static and dynamic mode I fracture toughness of rigid PUR foams under room and cryogenic temperatures. *Eng. Fract. Mech.* **2020**, *225*, 106274. [[CrossRef](#)]
74. Kathirvel, P.; Murali, G. Effect of using Available GGBFS, Silica Fume, Quartz Powder and Steel Fibres on the Fracture Behavior of Sustainable Reactive Powder Concrete. *Constr. Build. Mater.* **2023**, *375*, 130997. [[CrossRef](#)]

Disclaimer/Publisher’s Note: The statements, opinions and data contained in all publications are solely those of the individual author(s) and contributor(s) and not of MDPI and/or the editor(s). MDPI and/or the editor(s) disclaim responsibility for any injury to people or property resulting from any ideas, methods, instructions or products referred to in the content.